

THE PENNSYLVANIA STATE UNIVERSITY
COLLEGE OF EARTH AND MINERAL SCIENCES

DEPARTMENT OF GEOSCIENCES

**Reading Atmospheric and Biotic Influences in Soils: The Relationship Between Soil
Gas and Weathering Properties in Soils on Granite and Diabase**

A Senior Thesis in Geobiology

by

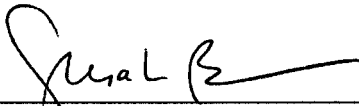
Reese J. Davis

Submitted in partial fulfillment
of the requirements
for the degree of

Bachelor of Science

Spring 2014

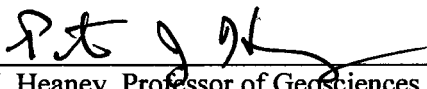
Reviewed and approved by:



Susan L. Brantley, Distinguished Professor of Geosciences
Director, Earth and Environmental Systems Institute

5-2-14

Date



Peter J. Heaney, Professor of Geosciences
Associate Head for Undergraduate Programs

5/2/14

Date

Reading Atmospheric and Biotic Influences in Soils: The Relationship Between Soil Gas and Weathering Properties in Soils on Granite and Diabase

Reese J. Davis

ABSTRACT

Carbon dioxide and oxygen concentrations in soils within regolith affect weathering and its formation, which is a unit that is a significant component of Earth's life-sustaining Critical Zone. Here, we examine CO₂ and O₂ gas concentrations in the soil atmosphere and study the atmospheric and biotic affects that influence gas concentrations and distributions throughout the soil profile. Bulk geochemistry, particle size, pH, and sulfur content is also measured and related to gas. This data was collected by installing gas sampling wells and taking samples throughout the Fall and Winter. Three sites were chosen, two of which were on diabase and one on granite in Pennsylvania (diabase) and Virginia (diabase and granite). Soil samples were collected from three sites via hand-auger or Geoprobe and analyzed in the laboratory. Soil CO₂ and O₂ were inversely related with depth. Clay content increased towards the surface displaying a more rapid increase in the profile where CO₂ concentrations began to deplete via consumption or more diffusive loss towards the surface. All soils became more acidic towards the surface. The shallowest profile (Virginia diabase) had the largest pH range, while the deepest profile (Virginia granite) had the smallest pH range. There was a decrease in sulfur content also with depth, however, the Pennsylvania diabase showed a significant increase in sulfur in its deepest sample. An interesting discovery was made when plotting O₂ versus CO₂. The Virginia granite and Pennsylvania granite had evidence of similar respiration and consumption rates of the gases, as indicated by the slope values of their trendlines, which were -0.9644 and -0.9817, respectively. The Virginia diabase had a much steeper slope of -2.2644. A slope of -1.0 means when one mole of O₂ is consumed, one mole of CO₂ is produced, so the Virginia diabase must have a lack of biotic activity at depth due to its slope, which translates to less O₂ consumption with less CO₂ production. Weathering can be visualized by the gas slope gradient, affecting particle size and oxide depletion. Soil pH decreases with the depletion of base oxides as the combination of gas and acidic rainwater weather regolith. Soil gas concentrations in regolith and characteristics of the soil on granite and diabase have broad similarities, but interesting differences even in a small region.

TABLE OF CONTENTS

Acknowledgements.....	i
Introduction.....	1
Experimental Methods.....	4
Results and Observations.....	7
Discussion.....	19
Conclusion.....	23
References Cited.....	24
Appendix.....	26

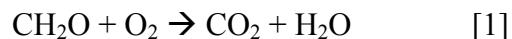
ACKNOWLEDGEMENTS

I would like to thank Gary Stinchcomb for advising and mentoring me throughout this entire process. His guidance and insight helped me learn and understand the skills and knowledge that made this project possible. I would also like to thank Susan Brantley for introducing me to the Critical Zone and providing thoughtful feedback on my work, Henry Gong for teaching me how to prepare samples to be run on ICP-AES and letting me use his facilities, Pamela Sullivan for taking the time out of her busy schedule to show me how to do sulfur titrations, Laura Liermann and Melanie Saffer for conducting my laboratory training and answering my questions while I did laboratory work, Joe Orlando and Tiffany Yesavage for troubleshooting laboratory problems and answering my questions while I worked in the laboratory, and also Penn State's Agricultural Analytical Services Lab for allowing me to use their facilities for particle size analysis. Lastly, I would like to thank funding from the DOE.

Introduction

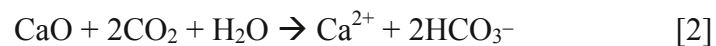
Regolith is the thin section of the Earth that extends from the soil surface to the parent bedrock (Brantley et al., 2013). Scott and Pain (2008) explain that it is essentially “everything from fresh rock to fresh air”. Regolith sits atop the crust and is formed by the weathering process where material is reequilibrated throughout the profile (Brantley et al., 2013). Organisms catalyze this weathering process from chemical and physical reactions that alter the material, which creates a chemical depth gradient that is associated with depth gradients of $p\text{CO}_2$ and $p\text{O}_2$ (Brantley et al., 2013). Regolith is a main component of the Critical Zone, or Earth’s thin, outer region that holds soils, groundwater, vegetation, etc (Brantley et al., 2007).

Today, there is a significant flux of CO_2 into the atmosphere because topsoils have higher CO_2 concentrations (Brook et al., 1983; Oh et al., 2005). Within regolith, CO_2 concentrations generally increase with depth, while O_2 concentrations generally decrease with depth for soils with biotic activity. Autotrophic and heterotrophic respiration in the form of microbes and roots, respectively, are the main producers of CO_2 in the soil atmosphere (Breecker et al., 2009). The ways in which soil biota interact with regolith makes this a large pool for carbon sequestration (Scott and Pain, 2008). This respiratory process, as expressed in equation [1], oxidizes organic matter to CO_2 producing water as a byproduct (Gulliver et al., 2010).



In abiotic soils, which are those influenced minimally by biotic activity, there will be a constant decrease in O₂ with depth as well as a constant decrease in CO₂ because rock weathering is the main consumer of both gases (Brantley et al., 2013).

Carbon dioxide is consumed in soils by a few means. Atmospheric inputs like precipitating rainwater is the main contributor to mineral dissolution, which in turn weathers rock by consuming CO₂ to form a weak acid (Scott and Pain, 2008). When CO₂ dissolves in water the pH of the solution is lowered and the rate of mineral dissolution increases because of the water's acidic state (Scott and Pain, 2008). In silicate rocks, the most important weathering acid is carbonic acid. Carbonic acid is dissociated to bicarbonate or carbonate ions by dissolution of alkali and alkaline earth element oxides (Holland and Zbinden, 1988; Pinto and Holland, 1988). Oxides dissolve in CO₂ and water to fix two moles of CO₂ to form bicarbonate in equations [2] and [3]:



Soils are subject to varying ranges in pH depending upon the mineral constituents of the parent material.

Granites with higher Si content have a lower CO₂ consumption capacity, while granites with lower Si content have a higher CO₂ consumption capacity. In the diabase, the two dominant minerals, plagioclase feldspar and pyroxene, create regolith high in Ca, Mg, Na, and K oxides, while in the granitic rock, these oxides comprise potassium and

plagioclase feldspar, which are high in oxides (Bazilevskaya et al., 2012; Pavich et al., 1989; Seiders et al., 1975).

Dissolution during weathering creates a decrease in these base oxides towards the surface, which has been observed in the Virginia Piedmont where there is almost a complete depletion in completely developed profiles (Brantley et al., 2013). Today these oxides are depleted at the reaction front, which lies between 0.7 and 1.0 m depth for diabase and ~2.5 and 20 m for granite (Brantley et al., 2013).

For O₂ consumption, Fe is the dominant consumer in rocks when there are small amounts of organic matter and sulfides. Equation [4] shows how ferrous oxide (FeO) reacts with O₂ to form ferric oxide (Fe₂O₃) (Holland and Zbinden, 1988).



Mafic rocks, like diabase, have a higher O₂ consumption capacity than felsic rocks, like granite (Brantley et al., 2013). The consumption of CO₂ is higher than O₂ consumption, more prominently at the surface, in both granite and diabase, however, overall, the consumption of CO₂ and O₂ are both inversely related with the concentrations of the oxides and FeO (Pavich et al., 1989 and Bazilevskaya et al., 2012).

The main focus of this paper is to interpret the effects of atmospheric influences in regolith in regards to soil gas and how this relates to bulk geochemistry and various soil characterization data. In this study, two diabase sites (DB1 & DB2) and one granite site (GR1) are examined. GR1 is located in Springfield, Virginia, DB2 is in Centreville, Virginia, and DB1 is in Carlisle, Pennsylvania.

Experimental Methods

Site Preparation

Gas samplers were fabricated in the laboratory for installation in the field using the US Geological Survey protocol by Schulz (2006). One-eighth inch stainless steel tubing was used with 0.2 mm openings. The wire tubing was cut into predetermined lengths and a mesh screen was glued to the bottom of each tube using Torr Seal® epoxy to prevent soil clogging. The sampling pieces of the gas well were also constructed in the laboratory. In the field, cores were collected from the granite (GR1) and diabase (DB1 & DB2) sites. Cores were collected using a hand auger and a Geoprobe on separate occasions. GR1 (VA Granite) was collected in October 2014, DB1 (VA Diabase) was collected in September 2014, and DB2 (PA Diabase) was collected in June 2014. Soil samples from various depths were packed in bags and labeled accordingly after collection via hand auger. Cores from the Geoprobe were fixed into five separate acetate sleeves. Gas samplers were installed within the boreholes for soil O₂ and CO₂ monitoring. A technique applying bentonite to cap and sand to fill the boreholes was used to complete the installation process. This technique is described by Schulz (2006).

Sample Characterization

Bulk soil chemistry of major elements was analyzed using inductively coupled plasma atomic emission spectrometry (ICP-AES, Perkin-Elmer Optima 5300). To prepare the samples for ICP-AES, samples were air-dried and subsamples were taken down to an appropriate size using a splitter. The samples were then powdered using a mortar and pestle and passed through a 100-mesh (149 microns) sieve. Next, 100 mg of

the each sample was mixed with 1 g of lithium metaborate. The mixture was then ready for analysis.

To determine loss on ignition (LOI), samples were powdered and put into pre-weighed ceramic crucibles. The crucibles with the samples were first put in an oven for 24 hours at 650°C. Next the samples were put in the oven for an additional 24 hours at 900°C. The weight of the crucible was subtracted by the total weight of the crucible and soil to determine the LOI.

Soil oxygen concentrations were analyzed using a Quantek O₂ analyzer performed at the field locations. Soil carbon dioxide concentrations were analyzed using a LI-COR CO₂ analyzer. Samples were collected with a syringe and sealed in vials at the field sites. Soil particle size analysis was conducted using the services at Penn State's Agricultural Analytical Services Laboratory. A hydrometer was used to determine clay content and a mechanical sieve was used to determine sand content.

Soil pH was determined using a method from the Soil Science Society of America by Thomas et al. (1996). Ten grams of air-dried soil was put into a 100 mL beaker. 10 mL of distilled water was added to the beaker and the mixture was stirred vigorously for 30 seconds. The mixture was then let sit for 5 minutes. An ORION Expandable ionAnalyzer EA 940 was used for this analysis using pH standards of 4 and 7. Between each measurement, the probe was rinsed with distilled water and dried. The measurement was recorded when the machine stabilized.

For sulfur analysis, the sulfur analyzer, LECO Induction Furnace, was used. To begin, 185 mL of water was boiled over a Bunsen burner. Separately, 2 g of starch were measured and dissolved into 15 mL of water. This starch solution was added to the

boiling water and then this entire mixture was cooled in a water bath to room temperature. After cooling, 6 g of c.p. potassium iodide (KI) were added to the mixture. At the LECO Induction Furnace, 1 N Hydrochloric Acid was added to the glass vesicle. The starch solution was squeezed to the indicated line and added to the glass vesicle and 0.100 gm/L KIO_3 was added until the dial read zero, which served as the starting value. For sample preparation, 510 to 515 mg of soil powdered to 100-mesh was added to the vestibule. Using a scooping instrument, 1 scoop of a tin metal accelerator and 2 scoops of an iron chip accelerator were added to the vestibule. Blanks consisted of only the accelerators, while standards consisted of the accelerators and a carbon/sulfur steel ring of 0.0079% sulfur. Two blanks and a standard were run before running samples. A blank was run between every 5 samples.

Results and Observations

Bulk Geochemistry

Major elemental concentrations for the GR1, DB1, and DB2 profiles decreased towards the surface. For profiles GR1 and DB1, the oxides generally show an overall decrease. Potassium oxide in DB1, however, increased in concentration toward the surface. In DB2, calcium oxide and magnesium oxide show an overall decrease toward the surface, but from 3.85 to ~1.3 m the concentrations reveal opposite trends of increasing and decreasing. The raw geochemical data is displayed in Table 1 (*Appendix*) and oxide concentrations versus depth are displayed in Figures 1a, 1b, and 1c.

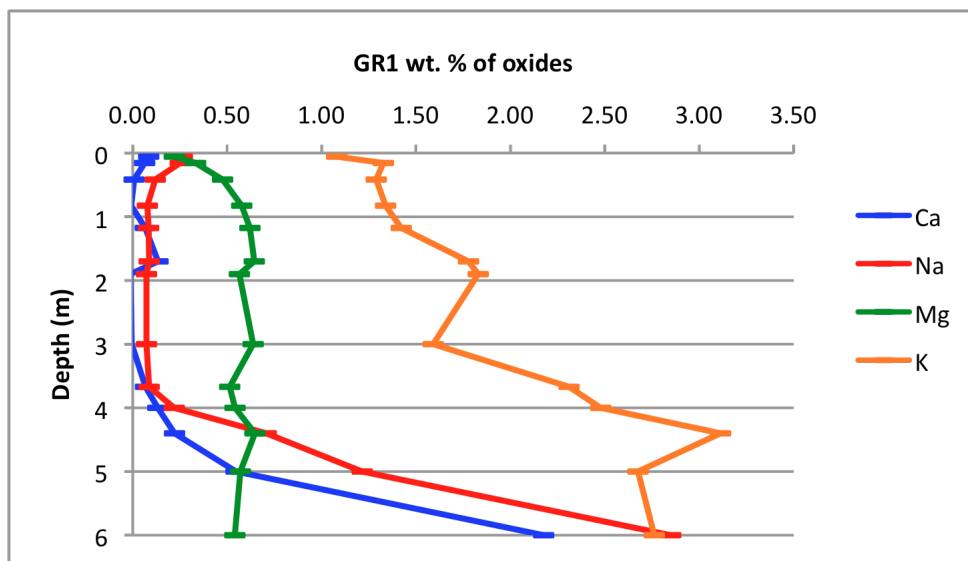


Figure 1a: GR1 (VA Granite) wt. % of oxide (Ca, Na, Mg, K) with depth

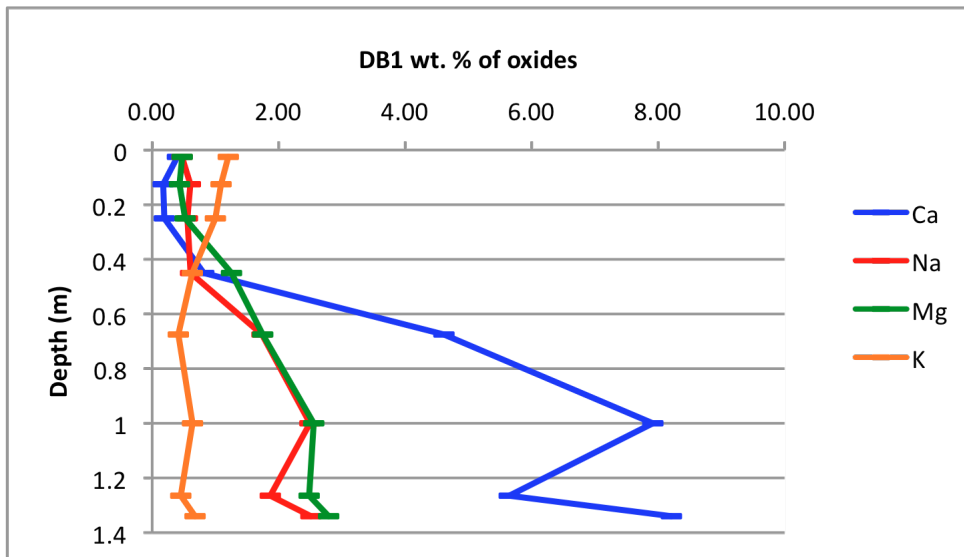


Figure 1b: DB1 (VA Diabase) wt. % of oxide (Ca, Na, Mg, K) with depth

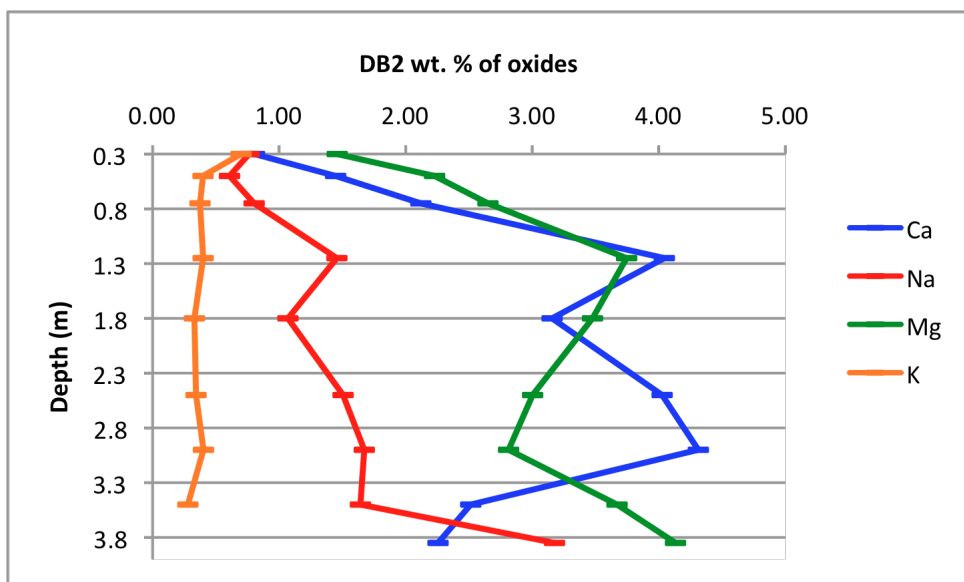


Figure 1c: DB2 (PA Diabase) wt. % of oxide (Ca, Na, Mg, K) with depth

Sulfur Analysis

Sulfur concentrations (*Figure 2*) were low at all sites. Each profile shows an overall decrease in sulfur with depth; however, the DB2 profile has an anomalous point at 3.85 m (red diamond). In the GR1 profile, sulfur concentrations are highest at 0.415 m and lowest at 7.17 m. From 0.055 m, concentrations increase significantly and peak at 0.415 m before decreasing with depth down to 7.17 m. Between 2 m and 3 m, the rate at which sulfur decreases appears to increase. In the DB1 profile, sulfur concentrations are highest at the shallowest depth, 0.025 m, and lowest at the deepest depth, 1.34 m. At 0.6 m, the rate at which sulfur decreases appears to increase. In the DB2 profile, sulfur concentrations are highest at the deepest depth, 3.85 m, and second highest at the shallowest depth, 0.3 m. This was the only profile that had the highest sulfur concentration at the deepest depth. Exact sulfur concentrations can be found in Table 2.

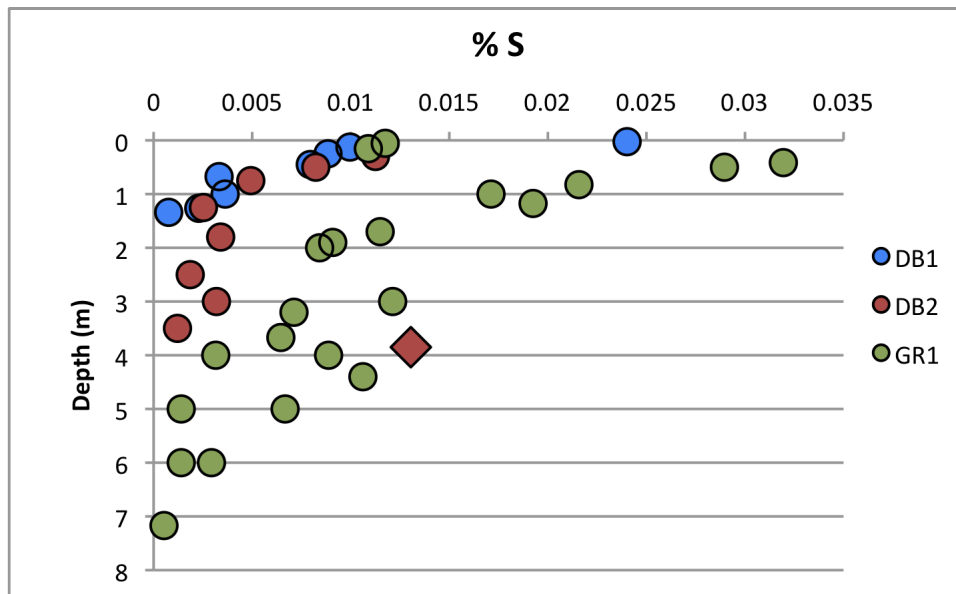


Figure 2: Percent sulfur in GR1 (VA Granite), DB1 (VA Diabase), and DB2 (PA Diabase) profiles. Red diamond is anomalous find in DB2.

GR1 Sample	Depth (m)	%S
GR1-0.055	0.055	0.01174863
GR1-0.155	0.155	0.01089152
GR1-0.415	0.415	0.03194565
GR1-0.825	0.825	0.02157585
GR1-1.175	1.175	0.01924891
GR1-1.70	1.7	0.01149086
GR1-1.90	1.9	0.00908679
GR1-3.00	3	0.01212622
GR1-3.67	3.67	0.00645374
GR1-4.00	4	0.00887534
GR1-4.40	4.4	0.01061622
GR1b-5.00	5	0.00666934
GR1b-6.00	6	0.00293405
GR1c-0.50	0.5	0.02895629
GR1c-1.00	1	0.01711634
GR1c-2.00	2	0.0084195
GR1c-3.20	3.2	0.00712063
GR1c-4.00	4	0.00315178
GR1c-5.00	5	0.00139916
GR1c-6.00	6	0.00139888
GR1c-7.17	7.17	0.00052591
DB1 Sample	Depth (m)	%S
DB1-0.025	0.025	0.02401906
DB1-0.125	0.125	0.00996107
DB1-0.25	0.25	0.0088434
DB1-0.45	0.45	0.00794621
DB1-0.675	0.675	0.00332005
DB1-1.00	1	0.00362837
DB1-1.265	1.265	0.00229237
DB1-1.34	1.34	0.00076427
DB2 Sample	Depth (m)	%S
DB2-0.3	0.3	0.01125445
DB2-0.5	0.5	0.00822699
DB2-0.75	0.75	0.00492849
DB2-1.25	1.25	0.0025259
DB2-1.80	1.8	0.00340049
DB2-2.50	2.5	0.00185645
DB2-3.00	3	0.00318608
DB2-3.5	3.5	0.00121041
DB2-3.85	3.85	0.01304839

Table 2: Sulfur concentrations for all profiles

Particle Size Analysis

Two particle size tests were performed on each profile. The first classified samples into percent sand, silt, clay, and textural class (*Table 3; Figures 3a, 3b, & 3c*) and the second classified samples into percent gravel, very coarse sand, coarse sand, medium sand, fine sand, very fine sand, and fines (*Table 4 in Appendix; Figures 4a, 4b, & 4c in Appendix*).

In GR1 at 0.055 m the texture is loam. Clay is present from 0.415 m to 1.175 m, which changes to clay loam from 1.70 m to 3.00 m. At 3.67 m it reverts back to loam until 5.00 m where it becomes sandy loam for the remainder of the profile. In the GR1 profile, there is an overall shift in grain size from sand to clay towards the surface, however, from 1.175 m to 0.055 m there is an increase in grain size back towards more sand content with an increase in silt at the surface.

In DB1 at 0.125 m the texture is clay loam. Clay is present from 0.25 m to 0.45 m, which changes to sandy clay at 0.675 m. Then from 0.75 m to the deepest sample at 1.34 m, there is loamy sand. In the DB1 profile, there is an overall decrease in grain size towards the surface, however, from 0.45 m to 0.125 m there is an increase in grain size with a higher silt content.

In DB2 there is a shift in texture from clay loam to clay to loam from 0.3 m to 0.75 m. Then there is loam from 1.25 m to 1.80 m, which shifts to sandy loam from 2.50 m to 3.00 m, before reverting back to loam for the remainder of the profile. In the DB2 profile there is a somewhat different trend. From 3.85 m to 2.5 m there is an increase in grain size, which then changes to a decreasing trend with clay formation, up until a slight increase in silt at the surface.

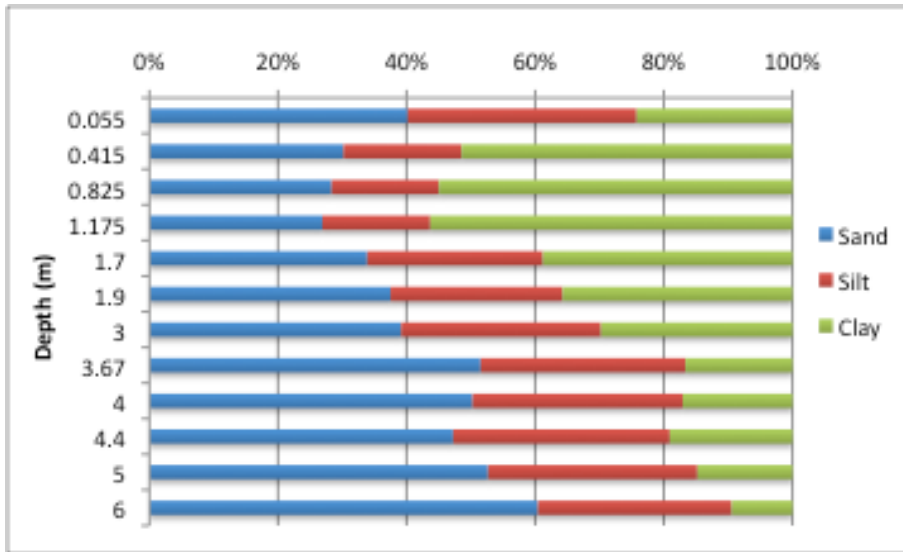


Figure 3a: GR1 (VA Granite) Profile depth vs % sand, silt, and clay

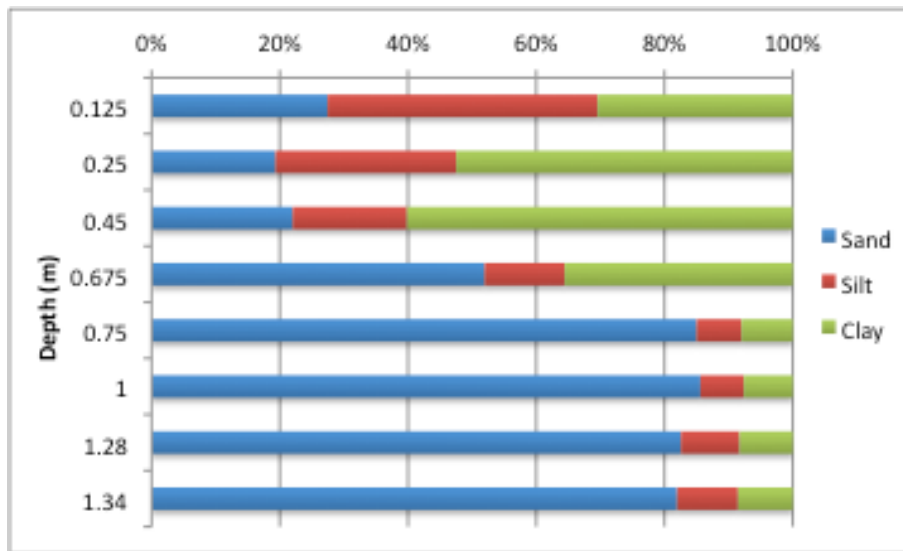


Figure 3b: DB1 (VA Diabase) Profile depth vs % sand, silt, and clay

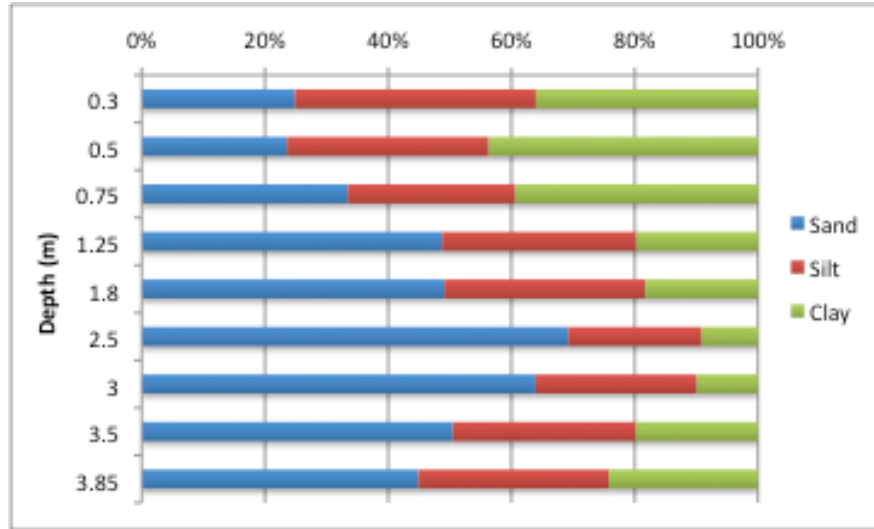


Figure 3c: DB2 (PA Diabase) Profile depth vs % sand, silt, and clay

GR1 Sample	Depth (m)	% Sand	% Silt	% Clay	Soil Textural Class
GR1-0.055	0.055	40.1621223	35.6177843	24.2200933	Loam
GR1-0.415	0.415	30.1812837	18.3733464	51.4453699	Clay
GR1-0.825	0.825	28.3420229	16.6840459	54.9739312	Clay
GR1-1.175	1.175	26.9029147	16.7750052	56.3220801	Clay
GR1-1.70	1.7	33.8797814	27.3224044	38.7978142	Clay Loam
GR1-1.90	1.9	37.5066881	26.7522739	35.741038	Clay Loam
GR1-3.00	3	39.1502591	31.0880829	29.761658	Clay Loam
GR1-3.67	3.67	51.5223881	31.840796	16.6368159	Loam
GR1-4.00	4	50.2552583	32.6730651	17.0716765	Loam
GR1-4.40	4.4	47.2402177	33.6874838	19.0722985	Loam
GR1b-5.00	5	52.6731753	32.5430033	14.7838215	Sandy Loam
GR1b-6.00	6	60.4275996	30.1263362	9.44606414	Sandy Loam
DB1 Sample	Depth (m)	% Sand	% Silt	% Clay	Soil Textural Class
DB1-0.125	0.125	27.4590164	42.1220401	30.4189435	Clay Loam
DB1-0.25	0.25	19.3307874	28.1869431	52.4822695	Clay
DB1-0.45	0.45	22.0130771	17.8323757	60.1545473	Clay
DB1-0.675	0.675	51.9323207	12.4975966	35.5700827	Sandy Clay
DB1-0.75	0.75	84.9969994	7.00140028	8.00160032	Loamy Sand
DB1-1.00	1	85.5956618	6.77851212	7.62582613	Loamy Sand
DB1-1.28	1.28	82.5697211	9.13014608	8.3001328	Loamy Sand
DB1-1.34	1.34	81.9631669	9.49307006	8.54376305	Loamy Sand
DB2 Sample	Depth (m)	% Sand	% Silt	% Clay	Soil Textural Class
DB2-0.30	0.3	24.8572287	39.0742411	36.0685302	Clay Loam
DB2-0.50	0.5	23.5679489	32.7565933	43.6754578	Clay
DB2-0.75	0.75	33.4333396	27.1891993	39.3774611	Clay Loam
DB2-1.25	1.25	48.7381703	31.5457413	19.7160883	Loam
DB2-1.80	1.8	49.1145939	32.5666599	18.3187462	Loam
DB2-2.50	2.5	69.2062044	21.669708	9.12408759	Sandy Loam
DB2-3.00	3	63.9054322	26.1685616	9.92600614	Sandy Loam
DB2-3.50	3.5	50.4787058	29.7127765	19.8085177	Loam
DB2-3.85	3.85	44.8776553	30.9222909	24.2000538	Loam

Table 3: Percent sand, silt, clay, and soil textural class for all profiles

Soil pH

Profile depth is correlated with pH range. All samples show an overall increase in pH with increased depth. The deepest profile, GR1, has the smallest increase in pH, while the shallowest profile, DB1, has the largest increase in pH. DB2 falls between GR1 and DB1 in both depth and pH range. GR1 shows the smallest increase, 0.93, DB2 shows an average increase, 1.64, and DB1 shows the largest increase, 3.04. Depth plotted versus soil pH for GR1, DB1, and DB2 is displayed in Figure 5 and exact soil pH values are in Table 5.

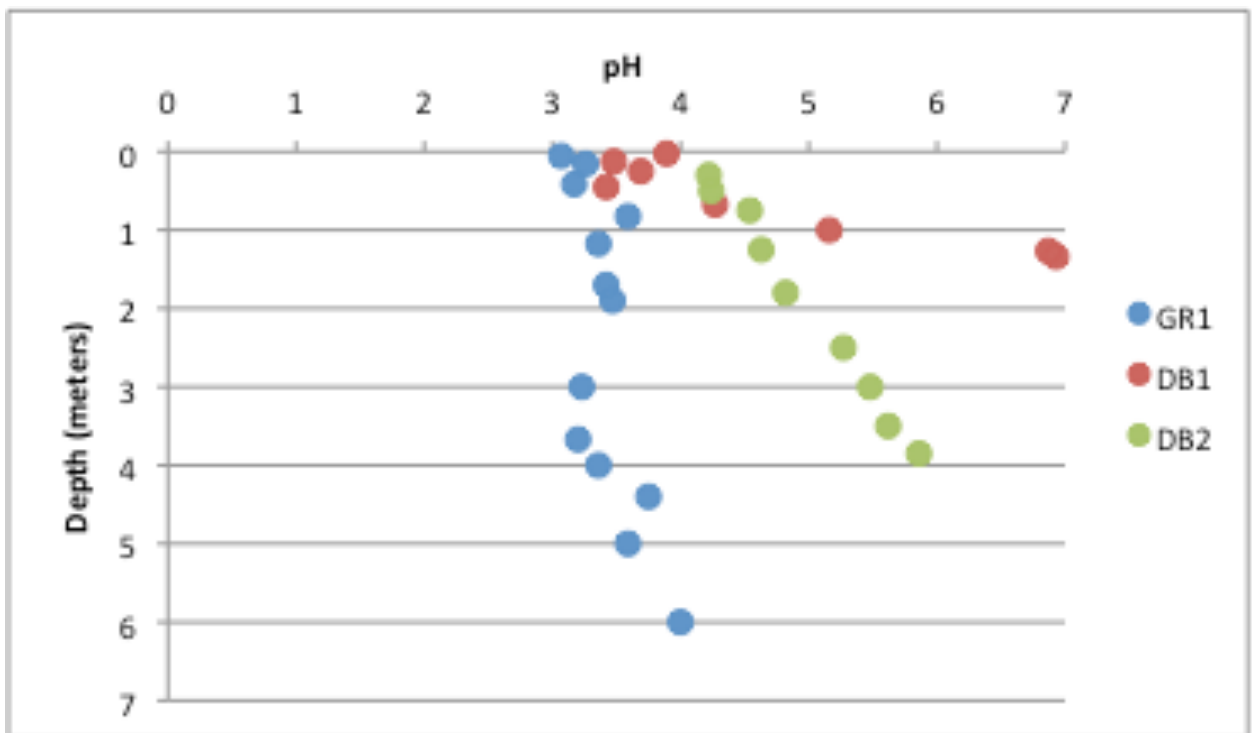


Figure 5: GR1 (VA Granite), DB1 (VA Diabase), and DB2 (PA Diabase) showing depth versus pH

Sample ID	pH (tenth)	pH (hundreth)
GR1-0.055	3.1	3.07
GR1-0.155	3.3	3.26
GR1-0.415	3.2	3.17
GR1-0.825	3.6	3.59
GR1-1.175	3.4	3.36
GR1-1.70	3.4	3.42
GR1-1.90	3.5	3.47
GR1-3.00	3.2	3.23
GR1-3.67	3.2	3.20
GR1-4.00	3.4	3.36
GR1-4.40	3.8	3.75
GR1b-5.00	3.6	3.59
GR1b-6.00	4.0	4.00
DB1-0.025	3.9	3.89
DB1-0.125	3.5	3.48
DB1-0.25	3.7	3.69
DB1-0.45	3.4	3.42
DB1-0.675	4.3	4.27
DB1-1.00	5.2	5.16
DB1-1.265	6.9	6.87
DB1-1.34	6.9	6.93
DB2-0.30	4.2	4.22
DB2-0.50	4.2	4.24
DB2-0.75	4.5	4.54
DB2-1.25	4.6	4.63
DB2-1.80	4.8	4.82
DB2-2.50	5.3	5.27
DB2-3.00	5.5	5.48
DB2-3.50	5.6	5.62
DB2-3.85	5.9	5.86

Table 5: GR1 (VA Granite), DB1 (VA Diabase), & DB2 (PA Diabase) with respective pH measurements to the tenth and hundredth

Gas Data

Overall, CO₂ increases with depth as O₂ decreases with depth for all three sites. GR1 has the largest change in CO₂ and O₂ concentrations throughout the profile, while DB1 has the smallest change. In DB2, the relationship between CO₂ and O₂ is prominently inversed and the lines break at the same depth with similar slopes. GR1 and DB2 display an elbow-like bend, with CO₂ and O₂ decreasing and increasing, respectively, at a distinct point in the profile. DB1 has a weaker elbow-like bend with a

less severe decrease in CO₂ and increase in O₂ at a point in the profile. Individual plots of depth versus percent gas by volume are displayed in Figures 6a, 6b, and 6c and actual gas concentrations can be seen in Table 6 in the Appendix. The gases were plotted against each other (O₂ versus CO₂). The slopes for GR1 and DB2 are -0.9644 and -0.9817, respectively, while the slope for DB1 is -2.2644. This relationship is shown in Figure 7.

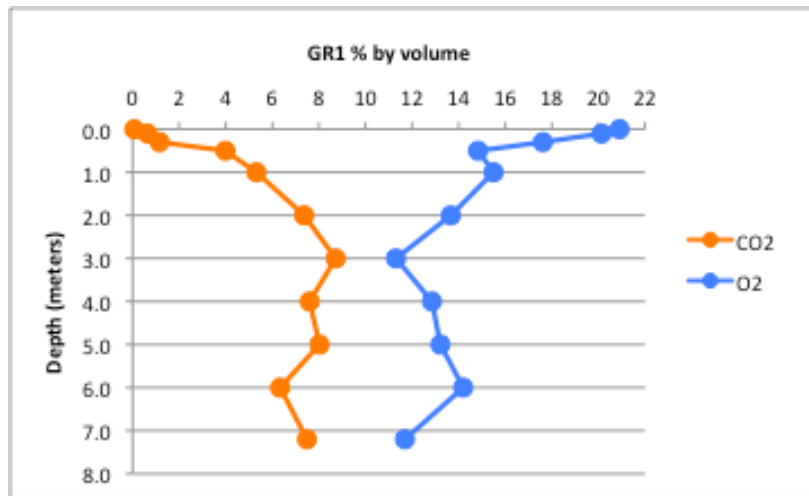


Figure 6a: GR1 (VA Granite) Gas Profile

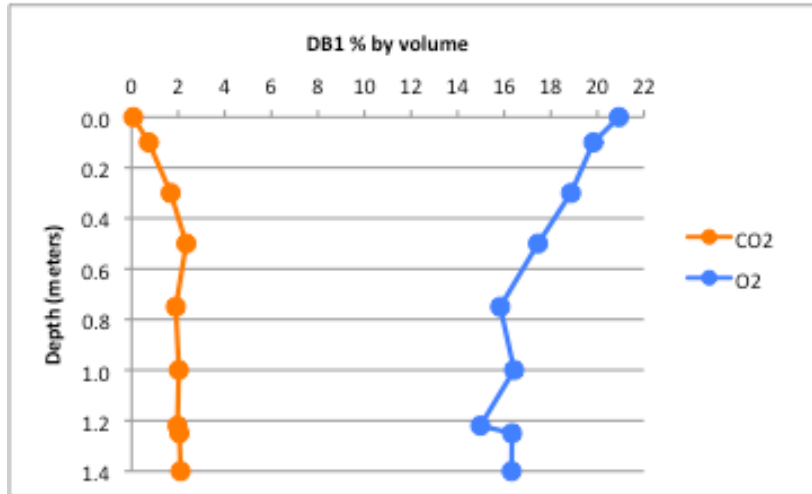


Figure 6b: DB1 (VA Diabase) Gas Profile

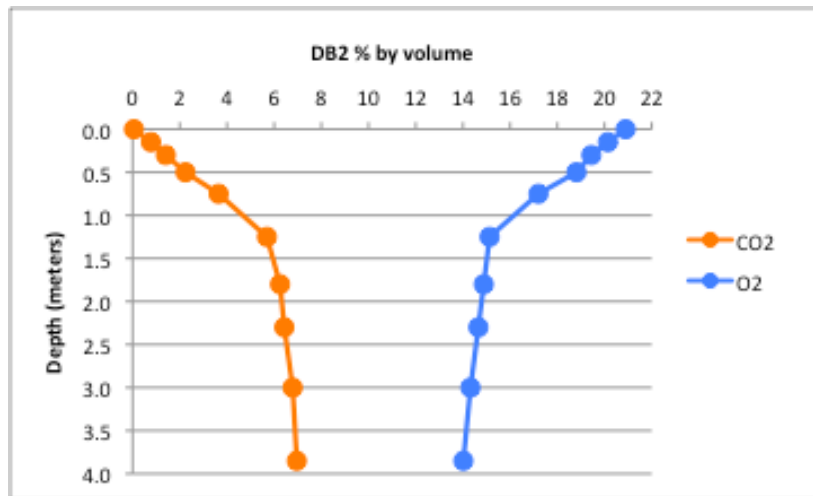


Figure 6c: DB2 (PA Diabase) Gas Profile

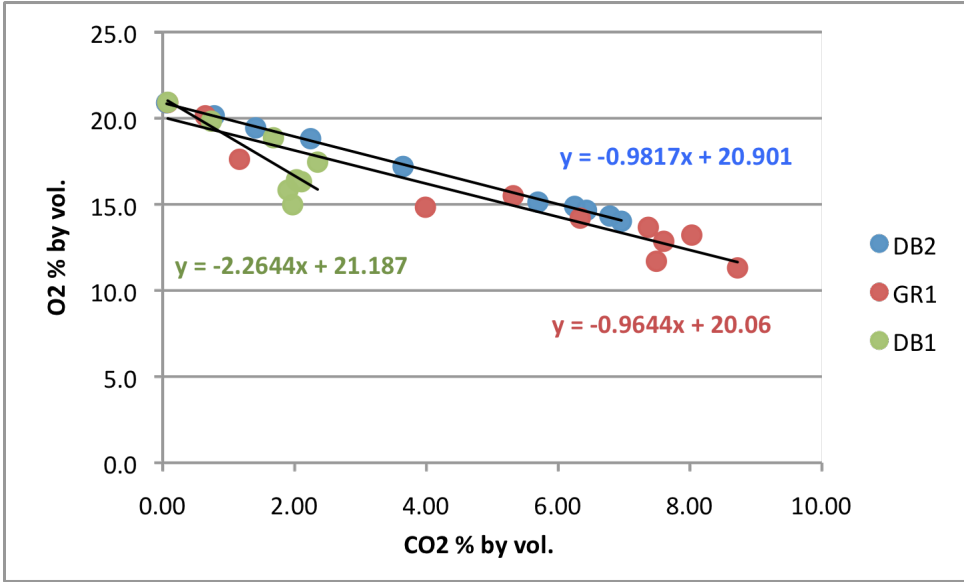


Figure 7: O₂ versus CO₂ for all profiles

Discussion

Particle Size

From depth towards the surface, grain sizes generally shift from high sand content to high clay content, with an increase in silt content at the surface. There is a low formation gradient of clay until a point in the profile where clay formation increases. This correlates with the concentration of soil gases, which promote weathering through oxidation (eq. 1) and dissolution (eq. 2 & 3). At depth, it is inferred that CO₂ is being respired by microorganisms as they intake available O₂ and make water. This CO₂ diffuses slowly at greater depths because of the fine clay material that exists in the B and C horizons. The diffusivity rate is therefore higher in the shallower, coarse-grained A and E horizons, allowing for the gas to escape more readily into the atmosphere (Richter and Markewitz, 1995). Carbon dioxide is unable to greatly weather rock and minerals because when CO₂ remains stagnant (and when it combines with water to form carbonic acid), weathering can only occur to a certain point until it is flushed out of the system and replaced with fresh CO₂ or carbonic acid with a capacity for weathering. This is referred to as a transport-limited system described by Brantley and White (2009). The slow rates at which water is flushed out of the system, therefore, affect the weathering rate.

Towards the surface is a point where the rate of clay formation increases and this correlates with the high rate of CO₂ consumption. At shallower depths, where heterotrophic biogenic activity is the highest, water is cycling through plants and there are more microorganisms and roots respiring O₂ and making CO₂. The higher biotic activity is due to microbe-rhizosphere interactions that force higher concentrations of

microorganisms near roots where they feed on organic material exudated from the plant roots (O'Neill, 1994). Here, we see an increase in clay content, which is associated with the drop in levels of CO₂. More CO₂ is being produced here than at lithogenic depths, but towards the surface the CO₂ can be lost to the atmosphere more quickly and be replenished with fresh water at a faster rate to produce carbonic acid, which in turn removes more CO₂ from the system.

A unique observation in DB2 gives the impression that a corestone might exist from around 4 to 1.5 m. Hausrath et al. (2011) observed this phenomenon in the Pennsylvania diabase at a quarry outcrop. Hausrath et al. noticed chemical weathering between corestones due to fractures that allowed for weathering around the stones. Because there is a bulge of high sand concentration “sandwiched” by clay zones, this could possibly be a corestone being weathering from the outside in. The clay layers would have been the layer where the fracture occurred.

Soil pH

For all three profiles, soil pH decreases towards the surface, and interestingly, the shallowest profile has the largest range in soil pH, while the deepest profile has the smallest change in soil pH because water is neutralized more rapidly in diabase than in granite. Rainwater is in an acidic state when it falls, containing carbonic (H₂CO₃) and sulfuric (H₂SO₄) acid. At the surface, regolith is more weathered than at depth and the surface area of mineral grains is much smaller than the larger, unweathered material below. Hydrogen cations in these acids react with the oxides in the soil by displacing the existing metal cation (Ca, Na, Mg, K). The metal cation is flushed out of the system and

now, with the proton in its place, the soil pH decreases. The soil pH for all profiles becomes more basic with depth because at depth there are more exchangeable cations.

The granite profile has only a small increase in soil pH with depth compared to the diabase profiles, which is due to the mineralogical makeup of the two rock types. Diabase has a higher concentration of oxides compared to granite. This increases the ability of diabase to neutralize acids as opposed to granite that has a high quartz content and smaller amounts of oxides. Because of this, the soil pH of GR1 increases just slightly from surface to depth compared to DB1 and DB2.

Sulfur

Sulfur concentrations at the top of the profiles show the highest levels. In forest ecosystems, sulfur comes from three sources: mineral weathering, atmospheric deposition, and organic matter decomposition (Edwards 1998). Currently, human activities account for approximately 50% of sulfur deposited into soils (Kennedy 1986). Organic sulfur, sulfur from leaf and plant litter, is largely immobile, while inorganic sulfur, sulfur from anthropogenic inputs, is largely mobile, especially sulfate (Edwards 1998). Emissions from burning coal are the primary source of atmospheric sulfur, which is oxidized to sulfur dioxide (Kennedy 1986). In the granite and diabase sites studied, atmospheric deposition is likely the main contributor to sulfur in the profiles. This is hypothesized due to the fact that sulfur decreases with depth, making it a mobile element and characteristic of inorganic sulfur, unlike immobile organic sulfur. Also, Pennsylvania has a history of coal emissions resulting in the production of sulfuric acid that falls as acid rain. This would be high in concentration at the top and deplete with depth as the acid interacts with weathered minerals and those less weathered minerals at depth.

In DB2 (Pennsylvania diabase), a significant increase in sulfur at the deepest point in the profile. In diabase, according to Sieders et al. (1975) and Pavich et al. (1989), the only sulfur-containing mineral present is pyrite, therefore, this must be pyrite that is quickly depleted (Bazilevskaya et al., 2012).

Soil Gas

As expected with increased depth, concentrations of CO₂ increased while O₂ decreased. The concentrations of these two gases tend to be inversely related because as one mole of O₂ is consumed, one mole of CO₂ is respired (equation 1). Slow rates of diffusion keep CO₂ concentrations high at depth compared to towards the surface even though there is a greater production of CO₂ at shallower levels. The shallower CO₂ is freer to interact with water and the atmosphere. The deeper, less weathered material is in that state because CO₂ has a certain weathering capacity, which is heightened by water interactions, but in both cases slow working due to high residence times. The biotic activity in soils triggered by oxygen from the soil atmosphere and organic matter creates an elbow-shaped CO₂ and O₂ trend with depth that bends at the point where the rate of weathering increases.

The plot with O₂ versus CO₂ (*Figure 7*) for the three profiles reflects the 1:1 ratio of consumption of O₂ and production of CO₂ due to the the slope values of the lines. GR1 and DB2 have slopes -0.9644 and -0.9817, respectively, which are both just under -1.0. The slop value for DB1 is -2.2644, indicating a steeper, negative slope, and a smaller concentration of CO₂ versus its respective concentration of O₂. This trend indicates that there must be less biotic activity in DB1 than GR1 and DB2 because oxygen is available, but it is not being consumed.

Conclusion

This study, and many others, show that soil gas is a product of biology and influenced heavily by additions from the atmosphere. In regolith, there is generally a depletion of oxides, increased acidification, and increased clay content towards the surface. The extent of these observations and characteristics is determined through weathering of regolith by soil gas and its interaction with material produced within the soil atmosphere and those added by the aboveground atmosphere. Further studies can examine the soils deeper on a biological level to gain a fuller grasp of the different biota that proliferate within different regolith of various bedrock types. For example, how do factors such as pH and particle size affect the activity of microorganisms and roots, which ultimately respire CO₂. The diabase profiles, DB1 and DB2, could also be further examined to determine the factors that contributed to the abiotic-like and biotic gas plots, respectively. An intricate blend of natural and anthropogenic influences creates a complex web of relationships that is the soil weathering system. Understanding the many components of this system that leads to regolith formation enhances our knowledge of the life-sustaining critical zone.

References Cited

- Bazilevskaya, Ekaterina, Marina Lebedeva, Milan Pavich, Gernot Rother, Dilworth Y. Parkinson, David Cole, and Susan L. Brantley. "Where Fast Weathering Creates Thin Regolith and Slow Weathering Creates Thick Regolith." *Earth Surface Processes and Landforms* 38.8 (2012): 847-58. Print.
- Brantley, S. L., M. B. Goldhaber, and K. V. Ragnarsdottir. "Crossing Disciplines and Scales to Understand the Critical Zone." *Elements* 3.5 (2007): 307-14. Print.
- Brantley, S. L., Lebedeva, M., and Bazilevskaya, E. (2013). Relating weathering fronts for acid neutralization and oxidation to pCO₂ and pO₂. In: Farquhar, J., Kasting, J., and Canfield, D. Eds.), *Treatise of Geochemistry, The Atmosphere -- History*. Elsevier Amsterdam, The Netherlands. Cahill J.A., Green R.E., Fulton T.L, Stiller M., Jay F., Ovsyanikov N, Salamzade R, St John J, Stirling I, Slatkin M, Shapiro B. 2013. Genomic evidence for island population conversion resolves conflicting theories of polar bear evolution. *PLoS Genetics* 9: e1003345.
- Brantley, S.L., White, A.F., 2009. Approaches to modeling weathered regolith. *Reviews in Mineralogy and Geochemistry* 70 (1), 435–484.
- Breecker DO, Sharp ZD, and McFadden LD (2009) Seasonal bias in the formation and stable isotopic composition of pedogenic carbonate in modern soils from central New Mexico, USA. *Geological Society of America Bulletin* 121: 630–640. <http://dx.doi.org/10.1130/B26413.1>.
- Brook GA, Folkoff ME, and Box EO (1983) A world model of soil carbon dioxide. *Earth Surface Processes and Landforms* 8: 79–88.
- Edwards, Pamela J. *Sulfur Cycling, Retention, and Mobility in Soils a Review*. Radnor, PA (5 Radnor Corp. Ctr., Ste. 200, Radnor 19087-4585): U.S. Dept. of Agriculture, Forest Service, Northeastern Research Station, 1998. Print.
- Gulliver, J.S., A.J. Erickson, and P.T. Weiss (editors). 2010. *Stormwater Treatment: Assessment and Maintenance*. University of Minnesota, St. Anthony Falls Laboratory. Minneapolis, MN.
- Hausrath, E.m., A.k. Navarre-Sitchler, P.b. Sak, J.z. Williams, and S.l. Brantley. "Soil Profiles as Indicators of Mineral Weathering Rates and Organic Interactions for a Pennsylvania Diabase." *Chemical Geology* 290.3-4 (2011): 89-100. Print.
- Holland HD and Zbinden EA (1988) Paleosols and the evolution of the atmosphere: Part I. In: Meybeck M and Lerman A (eds.) *Physical and Chemical Weathering in Geochemical Cycles*. New York: Kluwer Academic Publishers.
- Kennedy, I. R. 1986. Acid soil and acid rain: The impact on the environment of nitrogen and sulphur cycling. New York: John Wiley & Sons, Inc. 234 p.

Richter, Daniel D., and Daniel Markewitz. "How Deep Is Soil?" *BioScience* 45.9 (1995): 600. Print.

Oh N-H, Kim H-S, and Richter DD Jr. (2005) What regulates soil CO₂ concentrations? A modeling approach to CO₂ diffusion in deep soil profiles. *Environmental Engineering Science* 22: 38–45.

Pavich M, Leo GW, Obermeier SF, and Estabrook JR (1989) Investigations of the characteristics, origin, and residence time of the upland residual mantle of the Piedmont of Fairfax County, Virginia. U.S.G.S. Professional Paper 1352, U.S. Geological Survey 1–58.

Pinto JP and Holland HD (1988) Paleosols and the evolution of the atmosphere, part II. In: Reinhardt J and Sigleo W (eds.) *Paleosols and Weathering Through Geologic Time*, pp. 21–34. Boulder, CO: Geological Society of America.

Schulz, Marjorie. "Stonestrom Samplers: Nested Vertical Soil Gas Samplers A Primer for Installation and Handling." *US Geological Survey* (2006): n. pag. Print.

Scott, Keith M., and C. F. Pain. *Regolith Science*. Collingwood, Australia: CSIRO Pub., 2008. Print.

Seiders VM, Mixon RB, Stern TW, Newall MF, and Thomas JCB (1975) Age of plutonism and tectonism and a new minimum age limit on the Glenarm Series in the Northeast Piedmont near Occoquan. *American Journal of Science* 275: 481–511.

O'Neill, Elizabeth G. "Plant and Soil 1994, Volume 165, Issue 1, Pp 55-65 Responses of Soil Biota to Elevated Atmospheric Carbon Dioxide." *Plant and Soil* 165.1 (1994): n. pag. *Springer*. Oak Ridge National Laboratory. Web.

Thomas, G.W. 1996. Soil pH and Soil Acidity. In *Methods of Soil Analysis: Chemical Methods*. Part 3. D.L. Sparks, editor. Soil Sci. Soc. of Am., Madison WI.

Appendix

Profile	Sample ID	Depth (m)	Al ₂ O ₃ (%)	BaO (%)	CaO (%)	Fe ₂ O ₃ T (%)	K ₂ O (%)	MgO (%)	MnO (%)	Na ₂ O (%)	P ₂ O ₅ (%)	SiO ₂ (%)	SrO (%)	TiO ₂ (%)	LOI(900C)	
GR1	GR1-0.055	0.055	6.41	0.03	0.08	1.78	1.08	0.22	0.01	0.26	0.08	79.44	0.01	0.98	6.006	96.4
GR1	GR1-0.155	0.155	10.2	0.04	0.06	3.03	1.33	0.33	0.01	0.25	0.05	74.44	0.01	1.09	5.740	96.5
GR1	GR1-0.415	0.415	21.3	0.04	0.01	6.54	1.29	0.48	0.01	0.12	0.07	57.48	0.00	0.91	10.927	99.2
GR1	GR1-0.825	0.825	27.2	0.04	-0.01	7.89	1.34	0.58	0.01	0.08	0.04	46.08	0.00	0.67	16.990	100.9
GR1	GR1-1.175	1.175	27.5	0.04	0.07	7.99	1.42	0.62	0.01	0.08	0.08	47.92	0.00	0.67	13.978	100.4
GR1	GR1-1.70	1.7	25.0	0.05	0.13	5.77	1.78	0.64	0.01	0.09	0.06	55.04	0.00	0.54	11.061	100.2
GR1	GR1-1.90	1.9	25.1	0.05	-0.01	5.51	1.83	0.56	0.01	0.07	0.04	54.36	0.00	0.56	11.938	100.0
GR1	GR1-3.00	3	25.3	0.06	-0.01	4.86	1.59	0.64	0.02	0.07	0.03	54.33	0.00	0.54	12.195	99.7
GR1	GR1-3.67	3.67	18.0	0.09	0.07	3.18	2.31	0.51	0.06	0.09	0.09	66.6	0.00	0.32	n/a	91.3
GR1	GR1-4.00	4	19.2	0.09	0.13	3.77	2.48	0.54	0.04	0.22	0.08	64.1	0.00	0.39	n/a	91.1
GR1	GR1-4.40	4.4	23.1	0.09	0.22	4.40	3.11	0.65	0.03	0.71	0.09	57.53	0.00	0.49	9.295	99.7
GR1	GR1b-5.00	5	19.3	0.09	0.55	3.70	2.67	0.57	0.04	1.21	0.09	63.7	0.00	0.42	n/a	92.3
GR1	GR1b-6.00	6	19.6	0.09	2.18	3.17	2.76	0.54	0.04	2.85	0.06	63.6	0.02	0.41	n/a	95.3
GR1	GR1c-0.50	0.5	22.5	0.03	0.04	7.19	0.91	0.45	0.00	0.00	0.05	58.5	0.00	0.63	n/a	90.3
GR1	GR1c-1.00	1	24.5	0.03	0.04	6.04	1.03	0.48	0.00	0.00	0.05	57.0	0.00	0.67	n/a	89.8
GR1	GR1c-2.00	2	16.2	0.03	0.04	3.04	1.20	0.33	0.01	0.00	0.02	71.8	0.00	0.35	n/a	93.0
GR1	GR1c-3.20	3.2	18.9	0.08	0.10	3.83	2.43	0.57	0.02	0.08	0.05	64.9	0.00	0.42	n/a	91.4
GR1	GR1c-4.00	4	14.8	0.07	0.18	2.36	2.27	0.41	0.02	0.72	0.05	72.9	0.00	0.30	n/a	94.1
GR1	GR1c-5.00	5	17.3	0.09	0.53	3.01	2.54	0.64	0.08	2.22	0.08	67.6	0.01	0.34	n/a	94.4
GR1	GR1c-6.00	6	15.1	0.09	1.69	2.66	2.33	0.44	0.08	2.71	0.12	71.0	0.01	0.32	n/a	96.5
GR1	GR1c-7.17	7.17	13.5	0.07	1.70	2.31	2.13	0.39	0.03	2.62	0.04	76.0	0.01	0.29	n/a	99.1
DB1	DB1-0.025	0.025	6.36	0.04	0.40	4.66	1.20	0.47	0.16	0.47	0.11	71.86	0.01	2.30	12.660	100.7
DB1	DB1-0.125	0.125	7.47	0.03	0.17	3.85	1.09	0.43	0.10	0.60	0.06	79.33	0.01	1.97	4.893	100.0
DB1	DB1-0.25	0.25	8.21	0.03	0.19	4.83	1.00	0.52	0.08	0.56	0.06	74.76	0.01	2.19	7.867	100.3
DB1	DB1-0.45	0.45	16.4	0.02	0.82	9.83	0.63	1.25	0.03	0.61	0.02	58.68	0.01	1.23	11.799	101.4
DB1	DB1-0.675	0.675	19.2	0.03	4.61	9.32	0.41	1.75	0.14	1.74	0.10	49.30	0.02	0.74	14.586	102.0
DB1	DB1-1.00	1	20.1	0.04	7.92	7.99	0.64	2.55	0.11	2.49	0.16	52.33	0.03	0.97	6.637	102.0
DB1	DB1-1.265	1.265	18.2	0.04	5.64	9.34	0.45	2.48	0.12	1.87	0.09	50.05	0.02	0.78	12.088	101.2
DB1	DB1-1.34	1.34	19.2	0.04	8.21	7.83	0.68	2.79	0.11	2.51	0.18	52.77	0.03	0.89	6.024	101.3
DB2	DB2-0.30	0.3	16.7	0.04	0.81	9.97	1.36	1.46	0.16	0.76	0.16	57.19	0.01	1.16	12.763	102.6
DB2	DB2-0.50	0.5	19.3	0.03	1.45	12.66	0.70	2.23	0.18	0.61	0.08	45.66	0.01	0.83	18.234	102.0
DB2	DB2-0.75	0.75	21.0	0.02	2.12	13.22	0.40	2.65	0.18	0.80	0.06	44.47	0.01	0.68	16.615	102.2
DB2	DB2-1.25	1.25	19.7	0.02	4.04	11.47	0.37	3.75	0.16	1.46	0.11	46.82	0.01	0.65	12.088	100.6
DB2	DB2-1.80	1.8	20.2	0.02	3.16	12.17	0.40	3.48	0.17	1.07	0.09	46.51	0.01	0.66	14.154	102.1
DB2	DB2-2.50	2.5	21.8	0.02	4.03	9.96	0.33	3.00	0.14	1.50	0.10	46.06	0.02	0.55	14.174	101.7
DB2	DB2-3.00	3	21.7	0.02	4.31	9.61	0.34	2.81	0.13	1.67	0.10	46.96	0.02	0.56	17.038	105.2
DB2	DB2-3.50	3.5	19.2	0.02	2.51	11.67	0.40	3.67	0.15	1.64	0.07	44.14	0.01	0.65	17.038	101.2
DB2	DB2-3.85	3.85	18.1	0.01	2.26	11.06	0.28	4.13	0.14	3.18	0.09	48.28	0.02	0.55	13.595	101.7

Table 1: Raw geochemical data of samples from GR1, DB1, and DB2. The loss on ignition (LOI) is displayed as well.

Sample ID	% Gravel	% Very Coarse Sand	% Coarse Sand	% Medium Sand	% Fine Sand	% Very Fine Sand	% Fines
GR1-0.055	24.6593002	3.81237636	4.978297286	6.995525554	7.957872985	4.182509987	47.41411764
GR1-0.415	17.3262973	3.524062782	4.050646875	4.658243907	4.435458329	2.77469311	63.23059772
GR1-0.825	7.48847926	2.083679716	6.366799133	6.675492424	4.842626007	3.029052921	69.51387054
GR1-1.175	19.6602865	3.200785399	5.491873896	5.188641595	3.908327435	2.543782081	60.00630312
GR1-1.70	38.4390651	4.625480081	4.499330624	4.331131348	5.04597827	4.015757706	39.04325686
GR1-1.90	38.9646219	4.800535358	5.24140085	4.686236897	4.784207007	4.441311624	37.08168639
GR1-3.00	29.4049347	4.886787941	5.750022936	5.384245396	5.720760733	5.252565481	43.60068282
GR1-3.67	8.43672457	3.64430947	10.78715603	12.28132291	11.06047924	7.981037739	45.80897004
GR1-4.00	31.6534777	4.661576157	7.383155052	7.425025496	7.871643571	7.173802829	33.83131918
GR1-4.40	38.4285714	5.24928738	5.632214119	5.376929626	6.749083774	7.754266464	30.80964721
GR1b-5.00	33.8778626	6.53228926	6.547659352	5.932855657	7.469864895	9.083724595	30.55574364
GR1b-6.00	38.9550655	6.193480239	6.288399477	5.707019148	8.649515507	10.69027911	23.51624106
DB1-0.125	10.052981	2.805724408	2.908123109	1.535980515	4.566982066	4.853698429	73.27651045
DB1-0.25	17.5430778	0.899693641	1.049642581	0.67477023	2.849029862	3.268886894	73.71489895
DB1-0.45	29.890424	0.611218812	1.944787129	1.833656436	3.389486139	3.153333416	59.17709406
DB1-0.675	4.11119812	4.904137916	13.9749494	8.167417657	9.587036527	6.41593983	52.83932055
DB1-0.75	6.47061974	14.48124431	26.7547537	14.64963087	13.41479609	7.016106741	17.21284854
DB1-1.00	6.09855704	15.33994086	26.09699482	14.27378314	13.38266625	7.176673577	17.63138431
DB1-1.28	7.12316176	13.02804255	25.2543594	14.26146669	13.29014518	7.66264751	19.3801769
DB1-1.34	5.04972233	11.33923005	23.68799409	14.49402378	14.72837989	8.851449845	21.84920003
DB1-1.28	7.12316176	13.02804255	25.2543594	14.26146669	13.29014518	7.66264751	19.3801769
DB1-1.34	5.04972233	11.33923005	23.68799409	14.49402378	14.72837989	8.851449845	21.84920003
DB2-0.30	10.8626198	0.267921191	0.58942662	1.098476882	2.357706479	2.679211908	82.14463711
DB2-0.50	7.44746601	0.108830462	0.155472088	0.575246726	2.316534111	3.342649892	86.05380071
DB2-0.75	3.38051395	0.036234572	1.286327304	5.562006791	5.43518579	4.474969633	79.82476196
DB2-1.25	3.57042187	0.22814569	5.418460127	11.48333304	9.011754738	6.90140711	63.38647742
DB2-1.80	3.13050284	0.098584874	3.430753614	10.86405311	9.740185548	6.467167732	66.26875228
DB2-2.50	1.88619931	0.201419755	9.086268951	18.6648973	14.54698231	8.549149604	47.06508277
DB2-3.00	4.31848853	0.569841162	10.93058956	14.47051193	11.05146496	7.68422173	50.97488213
DB2-3.50	6.58189978	0.154206174	1.788791619	4.595343986	9.961718842	11.56546305	65.35257655
DB2-3.85	48.9966555	0.082285579	1.453711889	3.990850563	4.498278298	3.935993511	37.04222464

Table 4: In depth particle size distribution of GR1, DB1, and DB2

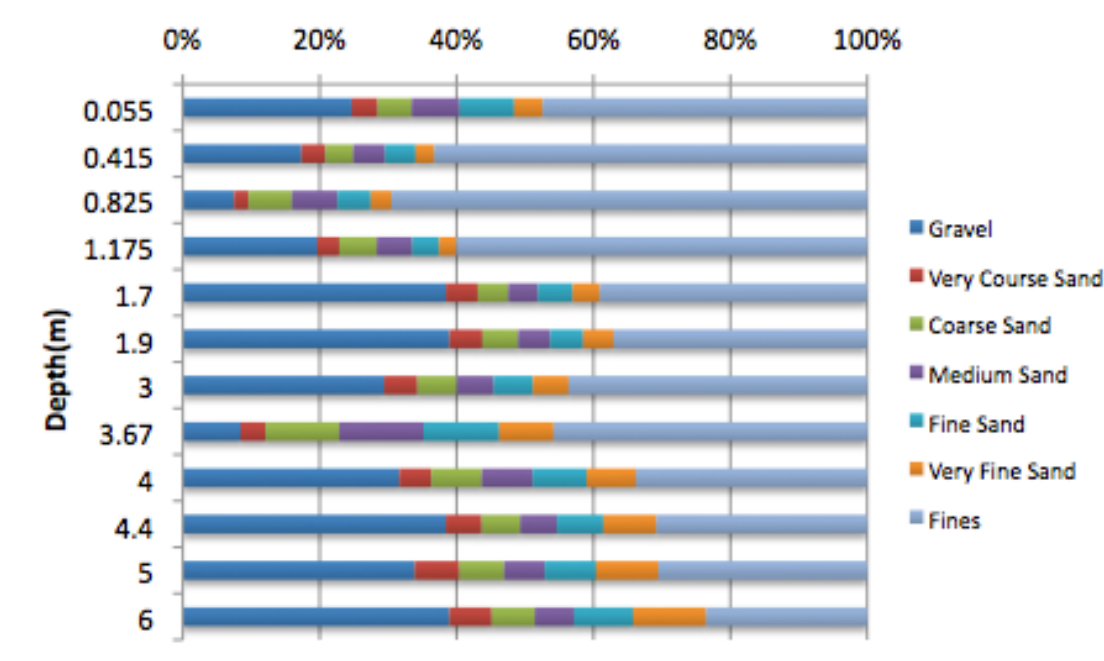


Figure 4a: In depth particle size distribution of GR1 (VA Granite)

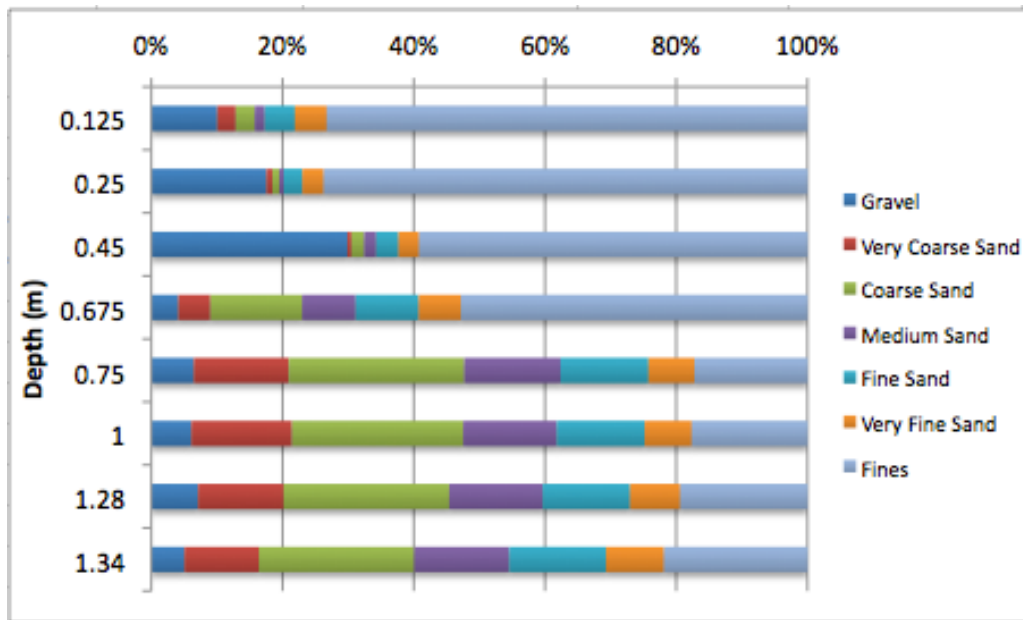


Figure 4b: In depth particle size distribution of DB1 (VA)

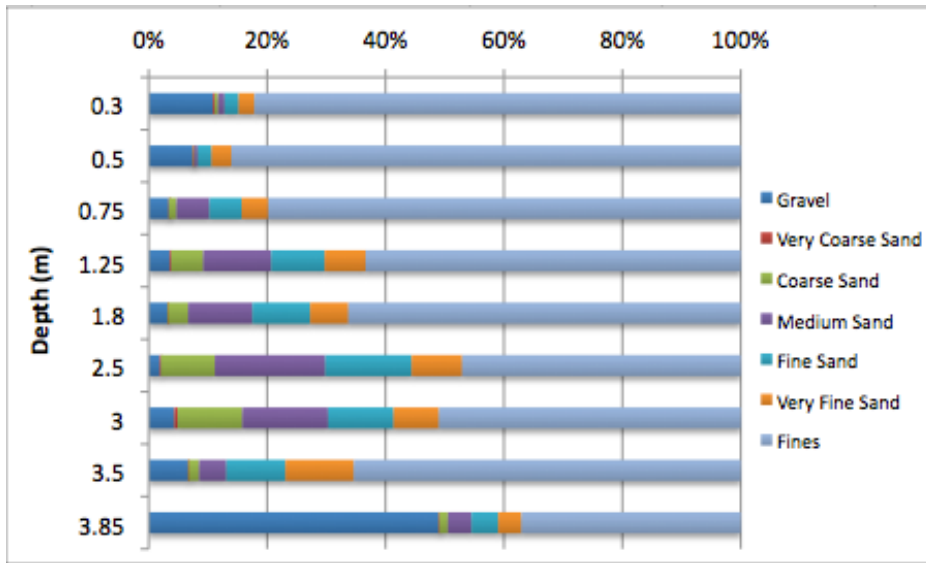


Figure 4c: In depth particle size distribution of DB2 (PA Diabase)

Site	Depth	CO2 % by vol.	O2 % by vol.
Granite (VA)	0	0.0752	20.913
Granite (VA)	0.1	0.6441	20.143
Granite (VA)	0.3	1.1628	17.617
Granite (VA)	0.5	3.9848	14.833
Granite (VA)	1	5.3174	15.500
Granite (VA)	2	7.3674	13.667
Granite (VA)	3	8.7217	11.311
Granite (VA)	4	7.6017	12.856
Granite (VA)	5	8.0271	13.217
Granite (VA)	6	6.3336	14.200
Granite (VA)	7.2	7.4901	11.696
Diabase (VA)	0	0.0737	20.925
Diabase (VA)	0.1	0.7366	19.830
Diabase (VA)	0.3	1.6786	18.867
Diabase (VA)	0.5	2.3490	17.452
Diabase (VA)	0.75	1.8997	15.829
Diabase (VA)	1	2.0283	16.428
Diabase (VA)	1.22	1.9700	14.978
Diabase (VA)	1.25	2.0528	16.336
Diabase (VA)	1.4	2.1044	16.317
Diabase (PA)	0	0.0573	20.895
Diabase (PA)	0.15	0.7803	20.143
Diabase (PA)	0.3	1.4089	19.442
Diabase (PA)	0.5	2.2426	18.813
Diabase (PA)	0.75	3.6458	17.200
Diabase (PA)	1.25	5.6927	15.131
Diabase (PA)	1.8	6.2492	14.882
Diabase (PA)	2.3	6.4295	14.655
Diabase (PA)	3	6.7843	14.321
Diabase (PA)	3.85	6.9590	14.018

Table 6: CO₂ and O₂ gas concentrations for GR1, DB1, and DB2